

See discussions, stats, and author profiles for this publication at: <https://www.researchgate.net/publication/40043998>

# Porphyrin–Cyclodextrin Conjugates as a Nanosystem for Versatile Drug Delivery and Multimodal Cancer Therapy

ARTICLE in JOURNAL OF MEDICINAL CHEMISTRY · DECEMBER 2009

Impact Factor: 5.45 · DOI: 10.1021/jm9007278 · Source: PubMed

CITATIONS

57

READS

113

7 AUTHORS, INCLUDING:



Jarmila Kralova

Institute of Molecular Genetics AS CR

74 PUBLICATIONS 1,172 CITATIONS

SEE PROFILE



Zdenek Kejik

Charles University in Prague

28 PUBLICATIONS 315 CITATIONS

SEE PROFILE



Tomás Bríza

University of Chemistry and Technology, Pra...

11 PUBLICATIONS 190 CITATIONS

SEE PROFILE



Vladimír Kral

University of Chemistry and Technology, Pra...

436 PUBLICATIONS 6,714 CITATIONS

SEE PROFILE

## Porphyrin–Cyclodextrin Conjugates as a Nanosystem for Versatile Drug Delivery and Multimodal Cancer Therapy

Jarmila Králová,<sup>†</sup> Zdeněk Kejík,<sup>‡,§</sup> Tomáš Bríza,<sup>‡,§</sup> Pavla Poučková,<sup>§</sup> Aleš Král,<sup>§</sup> Pavel Martásek,<sup>§</sup> and Vladimír Král<sup>\*,†,‡,⊥</sup>

<sup>†</sup>*Institute of Molecular Genetics, Academy of Sciences of the Czech Republic, Videňská 1083, 142 20 Prague 4, Czech Republic,*

<sup>‡</sup>*Institute of Chemical Technology, Prague, Technická 5, 166 28, Prague 6, Czech Republic,* <sup>⊥</sup>*Zentiva Development (Part of the sanofi-aventis Group), U Kabelovny 130, 10237 Prague 10, Czech Republic,* and <sup>§</sup>*First Faculty of Medicine, Charles University in Prague, Kateřinská 32, 121 08 Prague 2, Czech Republic*

Received May 28, 2009

The porphyrin–cyclodextrin conjugates were prepared and tested for selective and effective multifunctional drug delivery and therapy. The porphyrin receptor system combines efficient binding of the selected drug to the cyclodextrin cavity and photosensitizing properties of the porphyrin moiety with high accumulation of the whole complex in cancer tissue. The combined effect of chemotherapy and photodynamic therapy is demonstrated by *in vitro* and *in vivo* studies.

### Introduction

Many therapeutic methods such as chemotherapy, radiotherapy, photodynamic therapy (PDT<sup>a</sup>), and immunotherapy are used for treatment of cancer.<sup>1</sup> These methods can be used as single therapy or in combination with other therapeutic approaches; the latter strategy is called combined therapy. The advantage of the combined therapies is their higher therapeutic effect compared to the single therapy approach. The most favorable results are achieved when two or more different modes of treatment are applied simultaneously. For instance, Ladewig et al. have published a clinical study<sup>2</sup> on the successful combination of therapies utilizing parallel action of two drugs employing principles of photodynamic therapy (drug verteporfin) and chemotherapy (bevacizumab, mAb against vascular endothelial growth factor VEGF-A) for the treatment of neovascularization-related macular degeneration. Recently, several synergic photosensitizers integrating PDT and chemotherapy capabilities in one specifically designed agent have been developed.<sup>3,4</sup> Lunardi et al. have synthesized modified porphyrins producing the NO radical.<sup>3</sup> He et al. have tested a porphyrin inducing cancer cell apoptosis via DNA alkylation.<sup>4</sup>

Cancer chemotherapy is the major component of the modern oncologists' armamentarium. However, these drugs often show high toxicity for healthy tissues and low water solubility. These problems can be handled by targeted transport using a drug delivery system (DDS) such as cyclodextrins (CDs), cyclodextrin embodied systems,<sup>5</sup> and polymer conjugates.<sup>6,7</sup> The advantage of the DDS approach consists, in summary, of higher therapeutic effects of the delivered drug and decrease of the toxicity of systemic chemotherapy.

One of the most exploited areas of supramolecular nanomedicine in past decades has been the host–guest complexation of poorly soluble and orally administered drugs by

cyclodextrins, as they are the major class of macrocyclic organic host compounds. This is documented by more than 6000 published papers and approved patents. Incorporation of cyclodextrins into a drug dosage form first affects the activity of basic pharmaceutical ingredients by increasing their dissolution rate and bioavailability, and second, it modifies the properties of the whole prepared drug formulation by enhancing its stability, taste masking, binding, filling, channeling, osmogenic action, etc. Nearly 40 marketed commercial drug products currently benefited from such CD technology. Cyclodextrins, cyclic oligoglucose compounds, bear a hydrophobic cavity and a hydrophilic surface.<sup>8</sup> There are four basic types of cyclodextrins ( $\alpha$ ,  $\beta$ ,  $\gamma$ ,  $\delta$ ) with different numbers of glucose units. The ability of each cyclodextrin to form inclusion complexes with specific guests depends on a proper fit of the guest molecule into the hydrophobic cyclodextrin cavity,<sup>9</sup> which is given by steric dispositions and noncovalent binding capabilities. The steric fit depends on the relative size of the cyclodextrin with respect to the size of the guest molecule. Therefore,  $\alpha$ -cyclodextrin can typically complex low molecular weight molecules or compounds with aliphatic side chains,  $\beta$ -cyclodextrin can complex aromatic and heterocyclic molecules, and  $\gamma$ -cyclodextrin can accommodate even larger molecules such as macrocycles and steroids. Cyclodextrins and cyclodextrin systems have been tested for transport of many anticancer drugs<sup>10–12</sup> with suitable aromatic groups such as phenyl groups of paclitaxel. However, the binding constants are rather low, making cyclodextrins far from being an ideal vehicle for the drug transport; e.g., the  $K_s$  values for the complexes of  $\beta$ -cyclodextrin with paclitaxel<sup>13</sup> and  $\gamma$ -cyclodextrin with doxorubicin<sup>14</sup> (Figure 1) are  $3 \times 10^2$  and  $7 \times 10^2$ , respectively. The binding constant can be increased by linking two cyclodextrin units together to form a cyclodextrin dimer.<sup>15</sup> The host–guest interaction of substrates occupying both cavities is generally much stronger,<sup>16–18</sup> and the geometry of the resulting complex is better defined, since the substrate is grasped at both ends and held across the linker that ties the two cyclodextrins together.

PDT is a new treatment modality involving administration of a tumor-localizing photosensitizing agent (PS) followed by

\*To whom correspondence should be addressed. Telephone: +420 220 444 299. Fax: +420 220 444 058. E-mail: kralv@vscht.cz.

<sup>a</sup> Abbreviations: PDT, photodynamic therapy; VEGF-A, vascular endothelial growth factor; DDS, drug delivery system; CD, cyclodextrin; PS, photosensitizing agent; EPR, enhanced permeation and retention; TDD, targeted drug delivery.

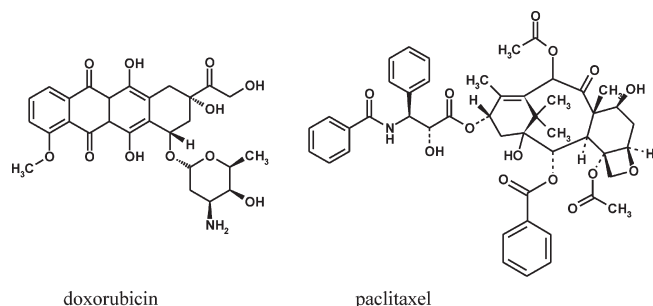


**Figure 1.** In vivo tested drugs.

activation of the agent by light of a specific wavelength resulting in a sequence of photochemical and photobiological processes that cause irreversible photodamage to tumor tissues. The successive cancer cell death is caused by oxidative stress because the photoactivation of PS results in the production of highly unstable singlet oxygen, which generates free radicals, thereby destroying the cell structures. In contrast to radiation therapy and chemotherapy, PDT has fewer adverse side effects and higher selectivity.<sup>19,20</sup> One group of PSs with high therapeutic potential is represented by porphyrins showing considerable selectivity for cancer cells and light absorption in the long visible region.<sup>21,22</sup> In addition, the light absorption of these PSs can be tuned up by expansion of the polyconjugated aromatic system. Because of their large aromatic structure, porphyrins have a tendency to aggregate. The formation of supramolecular oligomers can be an advantage, leading to an enhanced permeation and retention (EPR) effect. At appropriate ionic strength and/or acidity, porphyrins and their analogues can form highly ordered H- and J-type aggregates. In H-aggregates, the molecular components are stacked one-dimensionally in a “plane-to-plane” arrangement and a hypsochromic band appears in UV absorption spectra. In the case of J aggregates, strongly coupled monomers are self-assembled in an “end-to-end” manner to show a sharp peak at a red-shifted wavelength compared with that of monomers.<sup>23,24</sup> Because of a significant hydrophobicity of the porphyrin core, the solubility is enhanced by substitution with hydrophilic groups, e.g., hydroxyl,<sup>25</sup> sugar,<sup>26</sup> sulfate,<sup>27</sup> phosphonate,<sup>28</sup> cyclodextrin,<sup>29,30</sup> peptide,<sup>31</sup> and PEG.<sup>32</sup> The aggregation behavior of porphyrins is strongly dependent on their substitution.<sup>33</sup> Such modifications can also substantially influence the intracellular distribution of the PSs. For example, tetra(pentafluorophenyl)-porphyrin derivative aggregation was shown to be based on C–F...H–C interactions between fluorophenyl groups of one porphyrin to the pyrrole positions of a neighbor.<sup>33,34</sup>

In this work we have focused on the development of multifunctional porphyrin building blocks capable of creating molecular assemblies and accommodating various drug molecules. Our synthetic strategy combines the capability of CD to accommodate poorly soluble drugs and drugs with aromatic groups with the ability of modified porphyrins to function as efficient targeted drug delivery vehicles.

In order to achieve selective transfer of drugs into the cancer cells, we have developed porphyrin-cyclodextrin conjugates capable of noncovalent complexation of various cytostatic agents.

## Results and Discussion

In our strategy for targeted drug delivery, several current and important issues were addressed simultaneously: drug solubility, tissue selectivity, and multiple therapeutic actions.

**Table 1.** Logarithm Values of  $K_s$  for the Complexes Porphyrin-CD-Drug in Phosphate Buffer (1 mM) at pH 7.4 and 5.5

porphyrin-CD- drug complex	pH 7.34		pH 5.50	
	log( $K_s$ )	complex stoichiometry carrier/drug	log( $K_s$ )	complex stoichiometry carrier/drug
2-paclitaxel	5.3	1:1	nd	nd
2-docetaxel	6.3	1:1	5.1	1:1
	14.0	2:1	8.8	2:1
2-imatinib	11.0	1:2	9.9	1:2
	7.2	1:1	4.2	1:1
2-lapatinib	4.8	1:1	nd	nd
2-lomustine	6.0	1:1	4.4	1:1
2-fluorouracil	4.5	1:1	3.2	1:1
	9.6	2:1	6.5	2:1
2-aminopterin	4.8	1:1	nd	nd
	9.3	1:2	nd	nd
2-methotrexate	10.1	1:2	nd	nd
3-doxorubicin	11.0	1:2	5.8	1:1
3-sunitinib	9.0	1:2	nd	nd
4-paclitaxel	13.0	1:2	12.5	1:2
4-imatinib	10.7	1:2	10.3	1:2

For that purpose the drug delivery system consisting of versatile and stable noncovalent inclusion complexes of a delivery agent and a drug has been designed. The versatility of the system is granted by the adjustability of cyclodextrin cavity size allowing accommodation of cytostatic agents of various sizes. New modes of transport for a variety of current antineoplastics classified according to WHO as alkylating agents, antimetabolites, taxanes, anthracycline antibiotics, platinum compounds, and tyrosin kinase inhibitors have been tested with main focus on model hydrophobic compounds, paclitaxel, and docetaxel together with water-soluble doxorubicin (Tables 1–3). Paclitaxel and doxorubicin are the most used and studied drugs in the field of DDS. Doxorubicin is a member of the anthracycline antibiotic family. It is a widely used cytostatic agent whose mechanism of action is based on DNA intercalation resulting in inhibition of the DNA/RNA synthesis. It also triggers DNA cleavage by topoisomerase II leading to cell death. Another selected drug from the taxane family is paclitaxel. The mechanism of its action is based on hyperstabilization of microtubules which leads to the arrest of cell division and cancer cell death.

The most efficient systems, where efficacy of the therapeutic effect is consistent with effective drug binding, were tested *in vivo*. Thus, we used porphyrin- $\beta$ -cyclodextrin conjugates **1**, **2**, **4** for paclitaxel delivery and porphyrin- $\gamma$ -cyclodextrin conjugate **3** for doxorubicin transport (Figure 2A).

These very flexible systems exhibit high potential for the employment in multiple therapies in the targeted drug delivery (TDD) mode. Herewith, a porphyrin macrocycle is decorated with functional groups not only improving water solubility but also accommodating the drug in question. Moreover, the polarity of an individual drug delivery system was balanced by proper selection of the number of CD units attached covalently to the porphyrin ring. Furthermore, the high accumulation of porphyrins and expanded porphyrins in the malignant tissue, which is a well-known phenomenon, supports the selectivity of the system. Unlike many covalent systems intended for TDD, which usually suffer from being very rigid and unable to meet current requests for flexibility, our supramolecular approach is based on specific and effective binding of drugs by noncovalent interactions. Finally, the

**Table 2.** Effect of Combined Treatment on the Induction of Cell Death Using Mouse Mammary Carcinoma Cells 4T1 in Vitro

drug or carrier–drug complex	drug alone	cell mortality $\pm$ STD (%)			
		dark	carrier–drug		
			effect 1: <sup>a</sup> drug alone/ carrier–drug in the dark	PDT	effect 2: <sup>a</sup> drug alone/ carrier–drug subjected to PDT
<b>2</b> (2.5 $\mu$ M)		4.0 $\pm$ 1.9		25 $\pm$ 4.3	
<b>4</b> (5 $\mu$ M)		6.5 $\pm$ 3.0		27 $\pm$ 4.7	
docetaxel (2 $\mu$ M)	9.3 $\pm$ 2.3				
<b>2</b> –docetaxel		15.3 $\pm$ 3.6	A	61.1 $\pm$ 8.3	S
<b>4</b> –docetaxel		15.8 $\pm$ 5.6	A	62.4 $\pm$ 13.2	S
paclitaxel (1 $\mu$ M)	10.9 $\pm$ 1.0				
<b>2</b> –paclitaxel		15.6 $\pm$ 5.4	A	55.1 $\pm$ 8.1	S
<b>4</b> –paclitaxel		18.7 $\pm$ 1.5	A	57.5 $\pm$ 5.3	S
fluorouracil (5–10 $\mu$ M)	8.9 $\pm$ 1.0				
<b>2</b> –fluorouracil		12.7 $\pm$ 2.3	A	47.0 $\pm$ 4.4	S
<b>4</b> –fluorouracil		17.3 $\pm$ 6.6	A	64.7 $\pm$ 7.7	S
cisplatin (5–10 $\mu$ M)	4.9 $\pm$ 0.3				
<b>2</b> –cisplatin		7.4 $\pm$ 1.0	I	44.2 $\pm$ 12.5	S
<b>4</b> –cisplatin		7.0 $\pm$ 4.3	I	60.0 $\pm$ 12	S
lomustine (5 $\mu$ M)	6.2 $\pm$ 2.3				
<b>2</b> –lomustine		6.2 $\pm$ 1.8	I	48.0 $\pm$ 12.7	S
<b>4</b> –lomustine		7.5 $\pm$ 5.3	I	61.4 $\pm$ 17.2	S
methotrexate (0.5 $\mu$ M)	22.9 $\pm$ 0.2				
<b>2</b> –methotrexate		15.5 $\pm$ 4.2	I	53.5 $\pm$ 2	S
<b>4</b> –methotrexate		12.2 $\pm$ 1.9	I	67.1 $\pm$ 2.1	S
aminopterin (0.5 $\mu$ M)	21.9 $\pm$ 1.9				
<b>2</b> –aminopterin		22.0 $\pm$ 2.8	I	63.5 $\pm$ 2	S
<b>4</b> –aminopterin		18.7 $\pm$ 2.5	I	67.7 $\pm$ 5.9	S
imatinib (5–10 $\mu$ M)	5.2 $\pm$ 2.4				
<b>2</b> –imatinib		7.2 $\pm$ 2.2	A	21.3 $\pm$ 4.0	I
<b>4</b> –imatinib		10.1 $\pm$ 4.4	A	33.2 $\pm$ 4.7	A
lapatinib (5 $\mu$ M)	6.6 $\pm$ 2.0				
<b>2</b> –lapatinib		8.0 $\pm$ 2.5	I	48.3 $\pm$ 5.3	S
<b>4</b> –lapatinib		8.0 $\pm$ 0.8	I	45.5 $\pm$ 5.5	S
<b>3</b> (5 $\mu$ M)		4.5 $\pm$ 1.1		25.0 $\pm$ 3.3	
sunitinib (5 $\mu$ M)	4.9 $\pm$ 0.6				
<b>3</b> –sunitinib		4.5 $\pm$ 1.9	I	13.5 $\pm$ 1.9	I
doxorubicin (1 $\mu$ M)	11.6 $\pm$ 2.9				
<b>3</b> –doxorubicin		8.5 $\pm$ 2.3	I	65.2 $\pm$ 5.7	S
thioguanine (5 $\mu$ M)	4.6 $\pm$ 2.7				
<b>3</b> –thioguanine		4.3 $\pm$ 0.5	I	39.3 $\pm$ 1.6	S

<sup>a</sup>To distinguish the additive, synergic, or inhibitory effect, independent two-sample *t*-test was used to evaluate the mean values of six to nine independent experiments as described by Zimmermann.<sup>42</sup> S, synergic effect; A, additive effect; I, inhibitory effect.

stacking of the porphyrin photosensitizers yielding oligomers under physiological conditions leads to a very significant enhanced permeation and retention (EPR) effect, which together with the known plasma protein binding of photosensitizers further improves tumor localization and therapy efficiency.

In our previous work<sup>29</sup> we have found high selectivity of porphyrin–CD conjugates used as photosensitizers and their strong photodynamic effectivity for destruction of cancer cells. Here, we have designed and prepared porphyrin–monocyclodextrin, porphyrin–biscyclodextrin, porphyrin–tetrakis- $\beta$ -cyclodextrin, and porphyrin–bis- $\gamma$ -cyclodextrin conjugates **1–4** (Figure 2A) and tested them for applications in DDS and combined therapy systems in vivo and in vitro. In principle, cyclodextrin units are able to accommodate cytostatic drugs and the porphyrin moiety acts as a tumor selective vehicle and at the same time as a powerful tool for photodynamic therapy (Figure 2B).

The following aspects affecting the efficacy of the combined therapy were studied: (a) number of CD units on the macrocycle periphery; (b) size of CD ( $\beta$  and  $\gamma$ ); (c) complexation efficacy for the drug in question; (d) influence of the aggrega-

tion behavior; (e) mechanism of drug release by competition and by pH changes (pH controlled aggregation); (f) plasma protein binding of the tested photosensitizers.

**Binding Study.** To evaluate the formation of the complexes, we measured the binding constants for the drugs with porphyrin conjugates **1–4**; the values are summarized in Table 1, and typical titration curves are shown in Figures 3 and 5. Evaluation of the binding efficacy is described in the Experimental Section.

Here, we report in detail the results for two model drugs, paclitaxel and doxorubicin, but the system is generally applicable because many other drugs can form inclusion complexes with  $\beta$ - and  $\gamma$ -CD. Our results demonstrate the formation of strong inclusion complexes of the porphyrin conjugates **1–4** with the tested drugs. The  $K_s$  values are sufficient for successful application of the porphyrin–CD conjugates as drug delivery systems.

In general, the binding might be mediated first by classical inclusion complexation and second by nonclassical complexation, where the drug is bound to the narrow opening of the CD cavity in cooperation with  $\pi$ – $\pi$  stacking of the aromatic drug with the macrocycle. The nonclassical

**Table 3.** Effect of Combined Treatment on the Induction of Cell Death Using Leukemic Cells K562 in Vitro<sup>a</sup>

drug or carrier–drug complex	cell mortality ± STD (%)				
	drug alone	carrier–drug			
		dark	effect 1: drug alone/ carrier–drug in the dark	PDT	effect 2: drug alone/ carrier–drug subjected to PDT
<b>2</b> (2.5 μM)		4.9 ± 1.8		20.6 ± 2.8	
<b>4</b> (5 μM)		8.4 ± 2.8		25 ± 2.9	
imatinib (5–10 μM)	8.9 ± 1.9				
<b>2</b> –imatinib		12.5 ± 3.7	A	33.1 ± 11.3	A
<b>4</b> –imatinib		10.8 ± 2.3	I	35.1 ± 8.2	A
cisplatin (5–10 μM)	8.1 ± 3.8				
<b>2</b> –cisplatin		4.8 ± 1.8	I	30.7 ± 15.2	A
<b>4</b> –cisplatin		10.1 ± 3.0	I	45.3 ± 10.7	S
methotrexate (5 μM)	7.7 ± 1.9				
<b>2</b> –methotrexate		9.3 ± 5.4	A	49.6 ± 3.3	S
<b>4</b> –methotrexate		9.3 ± 0.3	I	46.2 ± 4.3	S
aminopterin (5 μM)	7.4 ± 1.6				
<b>2</b> –aminopterin		6.2 ± 1.9	I	54.5 ± 10.9	S
<b>4</b> –aminopterin		7.0 ± 3.0	I	41.6 ± 9.5	S
<b>3</b> (5 μM)		6.9 ± 1.8		19.0 ± 5.3	
doxorubicin (1 μM)	11.6 ± 2.9				
<b>3</b> –doxorubicin		11.7 ± 3.1	I	69.5 ± 10.7	S
sunitinib (5 μM)	4.9 ± 2.3				
<b>3</b> –sunitinib		8.8 ± 1.9	I	8.7 ± 2.0	I
thioguanine (5 μM)	8.1 ± 0.4				
<b>3</b> –thioguanine		7.8 ± 0.9	I	50.3 ± 5.8	S

<sup>a</sup> The average of four independent experiments is presented. S, synergic effect; A, additive effect; I, inhibitory effect.

complexation was ruled out on the basis of our NMR study, as we did not observe a significant shift to higher field for the bound drug (for details see Supporting Information).

In order to obtain an efficient combined therapeutic effect, PDT should be coupled with an effective release mechanism of the drug in the targeted cells (tissue). This feature plays a vital role in our proposed TDD system. Indeed, we observed a strong dependence of the drug binding efficacy of our TDD systems on pH (Figures 4 and 5, Table 6).

The study showed that the aggregation of the porphyrin–CD conjugates in aqueous solution is pH dependent and different types of aggregates exist at neutral versus weakly acidic conditions (Figure 4 and Supporting Information). F···H and F···C noncovalent interactions among the porphyrin–cyclodextrin conjugates at neutral pH (7.34), pH corresponding to “normal” physiological conditions, do not lead to the drug liberation from the CD cavity. On the contrary, at acidic pH (5.5), environment typical for cancer cells, the C<sub>6</sub>F<sub>5</sub> group is inserted to the CD cavity, which results in drug release from the complex.

The change of the aggregation behavior affects the receptor ability for the drug complexation and the release mechanism. For example, the value of *K<sub>s</sub>* for the porphyrin conjugate **2** is higher at neutral pH than acidic pH, where *K<sub>s</sub>* is too low to be determined. In the case of the complex porphyrin–γ-CD<sub>2</sub> with doxorubicin (**3**–doxorubicin), the change of the complex stoichiometry was observed to be 1:1 at acidic pH (Table 1). The above-described phenomenon is influenced by pH; the stability of this complex in neutral pH is markedly higher than in acidic pH (Figure 5, Table 6).

Further support for the effective release of the drug was provided by in situ fluorescent microscopic studies demonstrating intracellular localization of doxorubicin and carrier **3** (Figure 6) after 30 min of incubation with cells. Doxorubicin alone displays nuclear localization as demonstrated by colocalization with nuclear probe Hoechst 33342

(Figure 6, panel A), and carrier **3** is mainly localized in lysosomes as shown by overlay with lysosomal probe Lyso-Tracker Green (Figure 6, panel B). In contrast, at identical conditions the red fluorescence of complex **3**–doxorubicin is mainly lysosomal (Figure 6, panel C) and appears in the nucleus after 1 h of incubation. The appearance of doxorubicin in the nucleus after 1 h suggests its release from the complex.

The change of aggregation, specifically for the bis derivative, as a function of pH is interpreted in this way: the porphyrin–CD conjugates can be assembled via pentafluorophenyl–pyrrole interactions (as described earlier<sup>33,34</sup>) or via an inclusion complex of the porphyrin–CD derivatives, where the assembling mode is via inclusion of the porphyrin phenyl group to the CD cavity of the neighboring porphyrin (such binding mode has been reported recently<sup>35</sup>). A schematic representation is given in Supporting Information (Figure S1).

For the bis derivatives we have found that the tested drugs are bound with high binding affinity at pH 7, while a dramatic decrease in affinity was observed at pH 5. In contrast, tetrakis receptors could not self-aggregate via pentafluorophenyl groups; therefore, the drug release mechanism depends solely on competitive inclusion formation within the cell (amino acid, nucleobases, DNA, proteins, tubuline). Therefore, in spite of our initial expectation that the highly substituted derivative **4** would be a better system than derivative **2**, this was not proved.

Another mechanism of drug release relies on competition with biological molecules. We have tested binding of aromatic amino acids (model Phe) to our receptors. *K<sub>ass</sub>* was found in the range 200–300 for aromatic AA, which allows the rationalization that the physiological concentration of AA is another cause for the drug release (Supporting Information).

**In Vitro and in Vivo Studies.** In order to show the versatility and efficacy of our “Lego type” multifunctional system, the



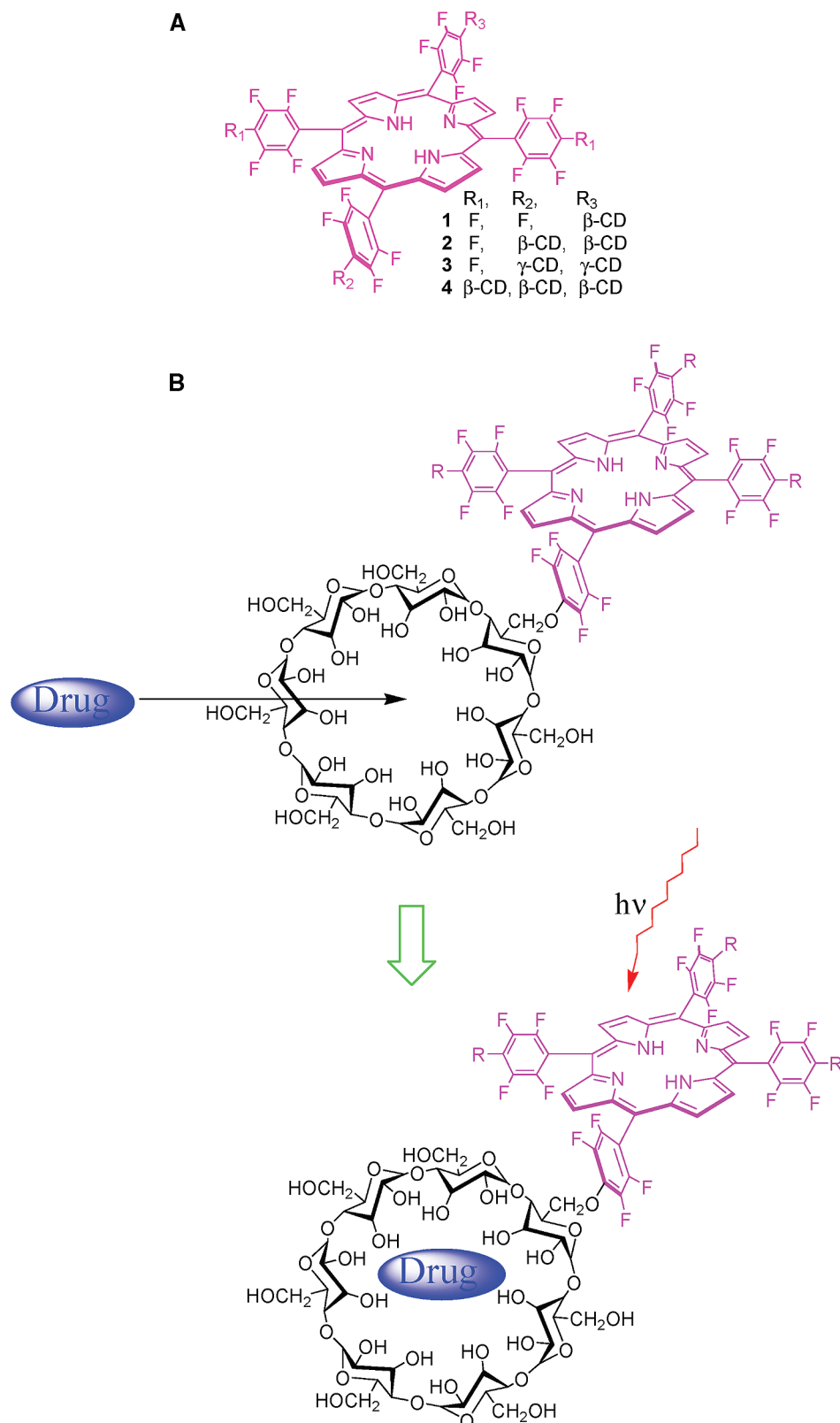


**Figure 2.** (A) Prepared and tested porphyrin–CD conjugates. (B) Schematic representation of formation of a supramolecular carrier–drug complex with dual therapeutic function.

drug alone or complexed with the porphyrin–CD was combined with photodynamic therapy. As a proof of the validity of the proposed principle, we first tested this system on tumor cells *in vitro*. Because of low binding affinity of monoderivative **1**, analysis was focused on derivatives **2–4**

and results are summarized in Tables 2 and 3. An important requisite for valid treatment is efficient drug complexation. The complexes of porphyrins **2–4** with particular drugs were formed during 1 h of incubation at room temperature and then added to cell cultures of mouse mammary carcinoma

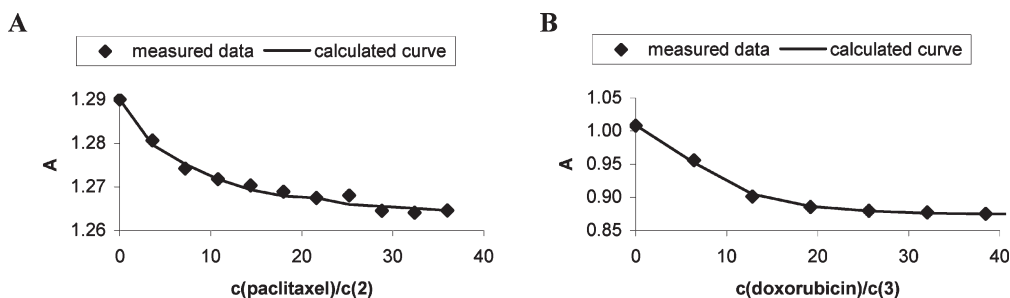


**Figure 3.** Titration curve of porphyrin derivatives with drugs in DMSO/water (2:98 v/v): (A) **2** and paclitaxel; (B) **3** and doxorubicin.

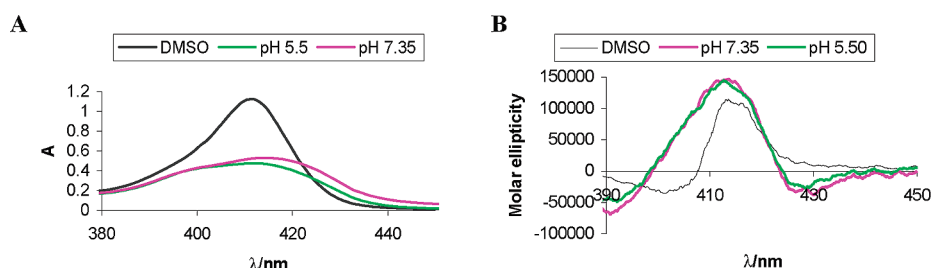


**Figure 4.** Spectroscopic analyses of pH dependence of aggregation for **2**: (A) absorption spectra of **2** ( $2.5\ \mu\text{M}$ ) measured in 1 mM phosphate buffer (DMSO/water, 2:98 v/v) at pH 7.35 and at pH 5.5; (B) circular dichroism spectra of **2** ( $2.5\ \mu\text{M}$ ) in 1 mM phosphate buffer (DMSO/water, 2:98 v/v) at pH 7.35 and at pH 5.5.

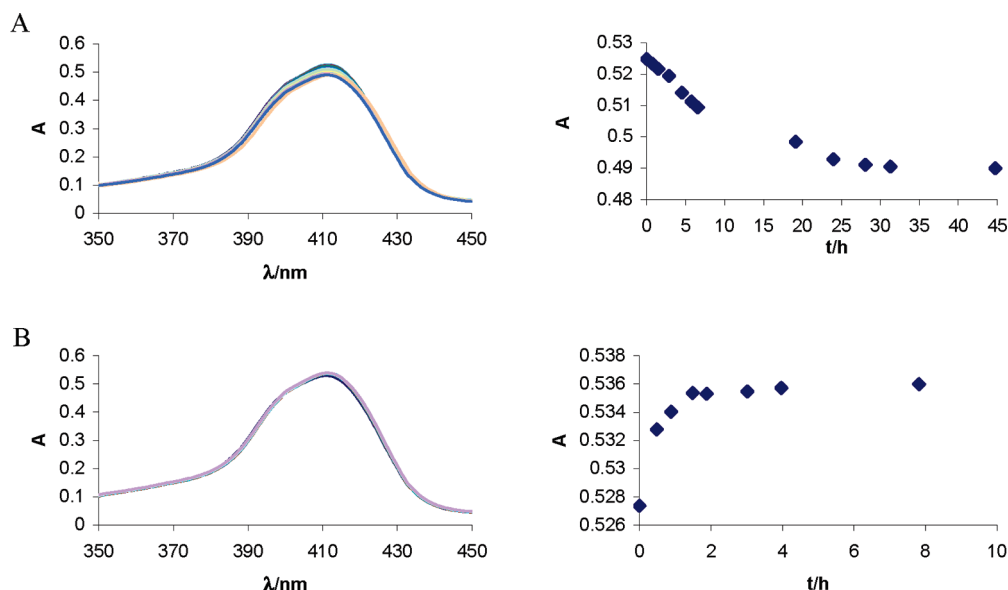


**Figure 5.** (A) Stability of complex **3** ( $2.5\ \mu\text{M}$ ) with doxorubicin ( $2.5\ \mu\text{M}$ ) in 1 mM phosphate buffer (DMSO/water, 2:98) at pH 7.34. (B) Stability of complex **3** ( $2.5\ \mu\text{M}$ ) with doxorubicin ( $2.5\ \mu\text{M}$ ) in 1 mM phosphate buffer (DMSO/water, 2:98) at pH 5.50.

cells, 4T1, or human chronic myelogenous leukemia cells, K562. Next day, cells were washed and exposed to light  $4\ \text{J}/\text{cm}^2$ . The mortality of the cells was monitored on the following day and evaluated as percentage of dead cells (Tables 2 and 3). The effect of unconjugated  $\beta$ -CD and  $\gamma$ -CD carriers complexed with drug was assayed in parallel to porphyrin-CD conjugates. The cell mortality of  $\beta$ -CD and  $\gamma$ -CD carrier/drug complexes (data not shown) and porphyrin-CD-drug complexes in the dark (without PDT) corresponded in most cases to the mortality induced by free drug. Only administration of complexes of porphyrin- $\beta$ -CD conjugates with lipophilic drugs (taxanes) resulted in 5–8% higher cell mortality in comparison to  $\beta$ -CD/drug, thus indicating that porphyrins likely facilitate solubility and/or

uptake of these drugs into cells. The concentration of each drug and PDT dose for porphyrin-CD conjugates was titrated to cause not more than 30% mortality by itself. In such conditions a synergistic effect of combined therapy was detected for most cytostatic agents carried by porphyrin-CD complexes except those inhibiting kinase activation (imatinib, sunitinib). As shown by our previous work, the inhibition of kinases is in conflict with the induction of PDT-mediated apoptosis.<sup>41</sup> The consistency of results obtained in 4T1 cells (Table 2) was also verified for cytostatic drugs used in clinics primarily against leukemic cells on K562 cells (Table 3). From these experiments it can be concluded that under in vitro conditions the combination of **2–4**-mediated PDT together with the drug delivery was much more

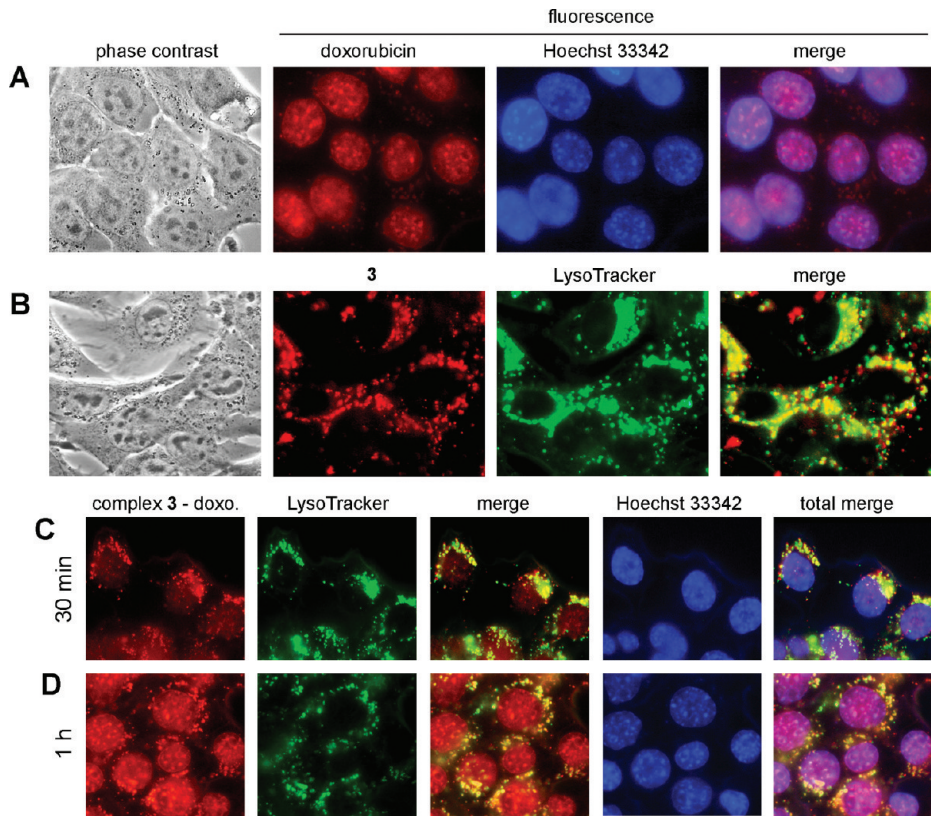


**Figure 6.** Doxorubicin release from the complex with porphyrin **3**. (A) Fluorescence images demonstrate colocalization of doxorubicin (red) with nuclear probe Hoechst 33342 (blue). (B) Colocalization of derivative **3** (red) with lysosomal probe LysoTracker Green (green). The corresponding images of their respective complex preformed in the tube and incubated with mammary carcinoma cells 4T1 for 30 min (C) and 1 h (D). The abundant presence of doxorubicin in the nucleus after 1 h indicates its release from the complex.

**Table 4.** Tumor Volumes 25 Days after One-Shot Therapy

tumor volume (treated group/control group) (%)			
carrier–drug complex	PDT	drug	carrier–drug subjected to PDT
2–paclitaxel	30	44	24
3–doxorubicin	44	54	32
4–paclitaxel	48	47	54

**Table 5.** Tumor Volumes 30 Days after Repeated Therapy

tumor volume (treated group/control group) (%)			
carrier–drug complex	PDT	drug	carrier–drug subjected to PDT
1–paclitaxel	29	exitus	29
2–paclitaxel	32	55	7, $P < 0.05$
3–doxorubicin	19	90	4, $P < 0.05$
4–paclitaxel	18	100	17

efficient in cancer cell killing than application of drugs or PDT alone.

Next, the therapeutic efficiency of our targeted drug transport together with PDT application was assayed on a mouse cancer model in vivo. BALB/c mice bearing subcutaneously growing mammary carcinoma, 4T1, received the respective photosensitizers **1–4** (5 mg/kg, iv) or their complexes with the appropriate drug at equimolar concentrations, and tumors in PDT-exposed groups were illuminated (100 J/cm<sup>2</sup>) 6 h after their administration. The tumor size was measured after one-shot therapy at regular intervals (Figure 7). Here, we show that the most efficient tumor

**Table 6.** Time Required for 50% Release of the Drug

carrier–drug complex	time (h)	
	pH 5.50	pH 7.34
2–paclitaxel	3	7
3–doxorubicin	1	13

growth reduction was observed in mice treated with **2** and **3** complexed with the drug and exposed to the light (Table 4). In contrast, the treatment of the animals either with the complexed drug without light engagement (chemotherapy) or exposed to the porphyrin-mediated PDT without the presence of the drug was less efficient, albeit the efficiency of PDT was higher than the efficiency of chemotherapy. Nevertheless, even in the case of the combined one-shot therapy the mice were not completely cured and tumor relapse occurred after 10 days. Therefore, we tested the potential of repeated therapy, where mice were exposed to a second dose of the treatment after 1 week. As demonstrated in Figure 8 and Table 5, the repeated therapy had a higher therapeutic effect than one-shot therapy. A very efficient and long-lasting effect of combined therapy was also obtained using the nude mouse model with human amelanotic melanoma C32 (Supporting Information, Figure S19).

**Additive or Synergic Effect of Combined Therapy in Vivo.**

On the basis of statistical evaluation, the synergic effect was confirmed for the repeated therapy using the combination of porphyrin–bis-CD derivatives **2** and **3** with the corresponding drug (paclitaxel and doxorubicin, respectively) (Table 5). Statistical evaluation (based on *t* test) showed the required



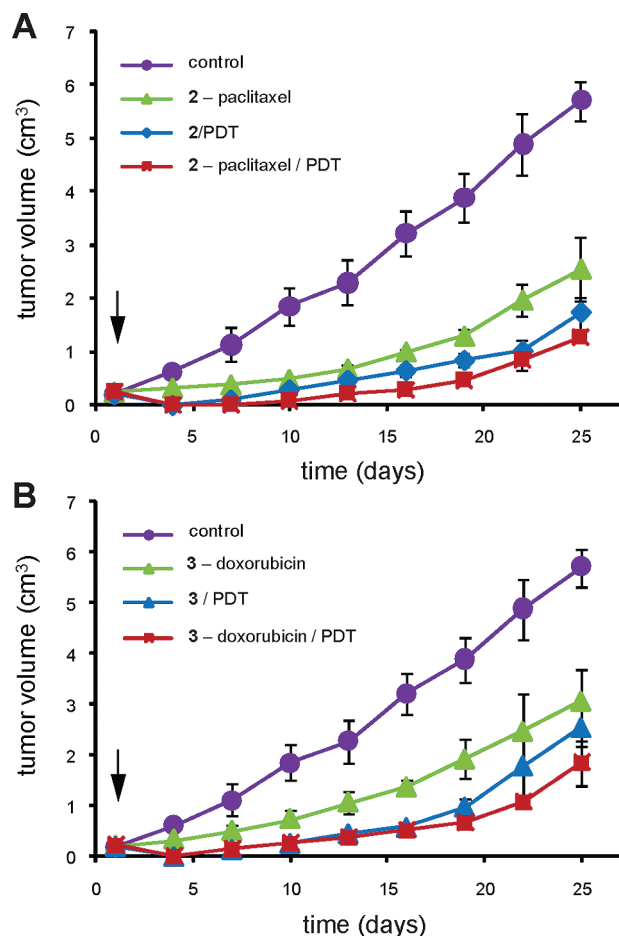


**Figure 7.** Influence of one-shot porphyrin-CD-drug mediated therapy on the growth of subcutaneous mammary carcinoma. Groups of mice ( $n = 8$ ) received **2** and **3** or their complexes with paclitaxel (A) and doxorubicin (B), respectively. Six hours later, the tumor area of PDT-exposed groups was illuminated with light dose  $100 \text{ J/cm}^2$ . The control group included mice without porphyrin and drug application. The effect of the delivered drug without PDT exposure is demonstrated by **2**-paclitaxel and **3**-doxorubicin.

confidence level ( $P < 0.05$ ; Table 5 and Supporting Information). However, for one-shot and for short-term therapies as well as in the case of mono- and tetra-CD derivatives only an additive effect was observed (Figures 7 and 8 and Tables 4 and 5). Thus, the combined therapy of the porphyrin-bis-CD derivatives **2** and **3** was clearly superior to the individual separated therapies.

Interestingly, while the tetrasubstituted derivative **4** was very efficient in combined therapy in vitro, its performance in vivo was not as good as the performance of bis-derivatives **2** and **3**. This difference is accountable to the drug release from the complex by the competitive inclusion formation with components present in the plasma before carrier/drug complexes can reach the tumor area.

In summary, bis derivatives **2** and **3** displayed PDT efficacy combined with potent drug complexation at physiological pH conditions and efficient release mechanism in cancer cells, thereby leading to more pronounced anti-tumor effect. This is documented by the model binding studies as well as by the outcome of in vitro application (Tables 2 and 3) and repeated therapy in vivo (Table 5, Figure 8).

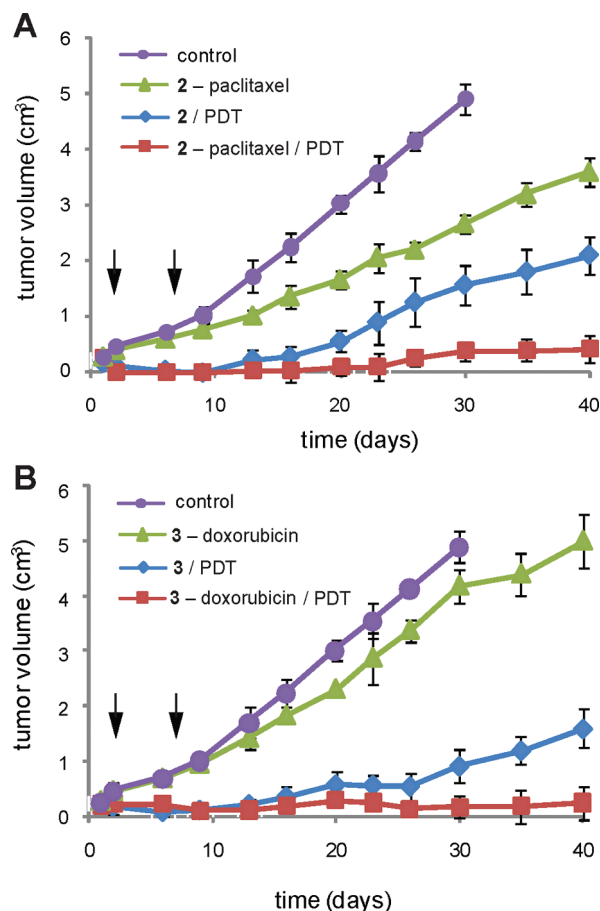


**Figure 8.** Influence of repeated porphyrin-CD-drug mediated therapy on the growth of subcutaneous mammary carcinoma. Groups of mice ( $n = 8$ ) received **2** and **3** or their complexes with paclitaxel (A) and doxorubicin (B), respectively. Six hours later, the tumor area of PDT-exposed groups was illuminated with light dose  $100 \text{ J/cm}^2$ . The treatment was repeated after 1 week. The control group included mice without porphyrin and drug application. The effect of the delivered drug without PDT exposure is demonstrated by **2**-paclitaxel and **3**-doxorubicin.

## Conclusions

In conclusion, we presented here a novel versatile supramolecular “Lego system” suitable for the combined cancer therapy, which is based on the effective drug binding as inclusion complexes with porphyrin-CD carriers **1–4** and on known tumor targeting by porphyrin macrocycles. The system allows very efficient combination of PDT with selective tumor accumulation and chemotherapy by cytostatic compounds. The described experiments demonstrate high potential of the combined therapy and justify further research in this direction leading to the desirable complete elimination of the tumor.

## Experimental Section

NMR spectra were recorded on Bruker 500 and Varian Gemini 300 HC (FT,  $^1\text{H}$  at 300 MHz,  $^{13}\text{C}$  at 75 MHz,  $^{19}\text{F}$  at 281 MHz) instruments using TMS and  $\text{CFCl}_3$  as the internal standards. Chemical shifts are quoted in ppm ( $\delta$  scale; s, singlet; bs, broad singlet; d, doublet; t, triplet; q, quadruplet; m, multiplet), and coupling constants  $J$  are in Hz. The solvent was DMSO. HPLC was performed with the LC 5000 HPLC system (INGOS, Czech Republic, by using CHROMuLAN program).

**Synthetic Strategy for Porphyrin-CD Conjugates.** The synthetic strategy was based on nucleophilic substitution of

tetrakis(pentafluorophenyl)porphyrin with the sodium salt of  $\beta$ - or  $\gamma$ -cyclodextrin. In the first step, cyclodextrin was converted into the corresponding sodium salt with sodium hydride; sodium salt was formed on primary hydroxyl group of C6 carbon.<sup>36,37</sup> Final nucleophilic attack to porphyrin provided a mixture of derivatives, monosubstituted and bis-, tri-, and tetra-substituted products. Substitution occurred in the para position of pentafluorophenyl ring. The starting ratio between porphyrin and cyclodextrin determined the major product of the corresponding nucleophilic substitution of the derivative. Thus, for example, the bis derivative was preferred over the mono-, tri-, and tetradervative when the ratio between porphyrin and cyclodextrin was 1:2. Bis derivatives can form two regioisomers. In the case of a smaller substituent, the substituent can be connected to the phenyl ring either in the 5,10 or the 5,15 position. The estimation can be done by <sup>1</sup>H NMR. As is described, in the region of  $\beta$ -pyrrole hydrogens of the 5,15-isomer (ABAB system), only two different signals (two doublets) appear.<sup>38</sup> In case of the 5,10-isomer (AABB system), the spectrum in this region is much more complicated, providing four different signals (two singlets and two doublets).<sup>39</sup>

In the case of large substituents such as cyclodextrins, bis derivatives are predominantly formed as 5,15-isomers (ABAB system).<sup>29</sup> In our strategy we have used  $\beta$ - and  $\gamma$ -cyclodextrins. In both cases we expected only isomer 5,15. The structure of porphyrin-bis-CD was determined from <sup>1</sup>H NMR spectrum. Two signals in the region of  $\beta$ -pyrrole hydrogens were observed, which is consistent with formation of the 5,15-isomer. This observation is in agreement with literature data.<sup>38</sup>

**Porphyrin- $\beta$ -CD<sub>1</sub> (1) and Porphyrin- $\beta$ -CD<sub>2</sub> (2).** Compounds **1** and **2** were prepared according to the procedure reported previously.<sup>29,40</sup>

**Porphyrin- $\gamma$ -CD<sub>2</sub>, 5,15-Isomer (3).** A flask was charged with 1 equiv of 5,10,15,20-tetrakis(perfluorophenyl)porphyrin (98 mg, 10 mmol) and 2 equiv of the sodium salt of  $\gamma$ -cyclodextrin (270 mg, 20 mmol) and dimethylformamide (10 mL). The mixture was heated under stirring at 50 °C for 12 h. Then the solvent was evaporated and the reaction mixture after washing by dichloromethane was applied (divided into several portions) to a 50 mL Supelco column (reversed-phase C18). The column was washed with methanol–water (gradient 5%, 20%, 50%, and 65%). Product **3** was eluted with water/methanol (25:75, v/v). The total yield of product **3** (porphyrin- $\gamma$ -CD<sub>2</sub>) was 34.7 mg (10%). <sup>1</sup>H NMR (DMSO)  $\delta$  -3.2 (bs 2H, NH), 3.2–3.9 (m, H-CD), 4.4–5.0 (m, H-CD), 5.5–6.0 (m, H-CD), 9.4 (splitting bs into d, 8H, Ar-py). <sup>19</sup>F NMR (DMSO)  $\delta$  -135.0 (m), -137.5 (m), -149.5 (m), -152.0 (m), -158.5 (m). MALDI-TOF calculated, 3528; found, 3527.595. Anal. Calcd for C<sub>140</sub>H<sub>168</sub>F<sub>18</sub>N<sub>4</sub>O<sub>80</sub>·2H<sub>2</sub>O: C 47.17%, H 4.86%, N 1.57%; found C 47.12%, H 4.92%, N 1.53%.

Solutions (200  $\mu$ g mL<sup>-1</sup>) of the porphyrins were prepared in distilled water, and an amount of 100  $\mu$ L of samples was injected onto the column. The column was equilibrated with 100 mL of the mobile phase prior to analysis, and the separations were performed in an air-conditioned room (26 °C). When the column was not in use, the mobile phase was replaced with the storage solvent recommended by the column supplier.

Separations were carried out on a Nucleosil C18 column (250 mm  $\times$  4.6 mm i.d., 5  $\mu$ m particle), with eluant acetonitrile–water (7:3) used as the mobile phase. The mobile phase flow rate was 0.5 mL min<sup>-1</sup>, and the wavelength was set to 400 nm. Retention time was 8.9 min.

**Porphyrin- $\beta$ -CD<sub>4</sub> (4).** A flask was charged with 1 equiv of 5,10,15,20-tetrakis(perfluorophenyl)porphyrin (98 mg, 1 mmol) and 8 equiv of the sodium salt of  $\beta$ -cyclodextrin (908 mg, 6.7 mmol) and dimethylformamide (12 mL). The mixture was heated with stirring at 90 °C for 6 h. Then the solvent was evaporated and the reaction mixture after washing by dichloromethane was applied (divided into several portions) to a 50 mL Supelco column (reversed-phase C18). The column was washed

with methanol–water (gradient 5%, 20%, 50%, and 65%). Product **4** was eluted with water/methanol (25:75, v/v). The total yield of product **4** (porphyrin- $\beta$ -CD<sub>4</sub>) was 108 mg (20%). <sup>1</sup>H NMR (DMSO)  $\delta$  -3.1 (bs 2H, NH), 3.1–3.8 (m, H-CD), 4.4–4.9 (m, H-CD), 5.5–5.8 (m, H-CD), 9.2 (bs, 8H, Ar-py). <sup>19</sup>F NMR (DMSO)  $\delta$  -142.0 (m), -156.7 (m). MALDI-TOF calcd, 5431; found, 5436.842 (M + Na - H<sub>2</sub>O), 5417.859 (M + Na - 2H<sub>2</sub>O). Anal. Calcd for C<sub>212</sub>H<sub>286</sub>F<sub>16</sub>N<sub>4</sub>O<sub>140</sub>·2H<sub>2</sub>O: C 46.55%, H 5.34%, N 1.02%; found C 46.61%, H 5.37%, N 0.99%. HPLC analysis: Nucleosil C18 column (250 mm  $\times$  4.6 mm i.d., 5  $\mu$ m particle); mobile phase, methanol (1:9) with (0.1% TEAA), pH 4; retention time was 7.9 min.

**Determination of the Binding Constants of the Drugs with the Porphyrin–Cyclodextrin Conjugates.** The association of the porphyrins (**1–4**) with the drugs was studied using UV–vis spectroscopy in water with 2% DMSO. Binding constants ( $K_s$ ) were calculated from absorbance changes of the porphyrins using Soret band maximum ( $\Delta A$ ) by nonlinear regression with the program Letagroup Spefo 2005. Concentration of the used porphyrins was  $5 \times 10^{-6}$  mol/L, and concentration of the drugs varied from  $10^{-6}$  to  $10^{-4}$  mol/L. Hydrophobic drugs were dissolved in a small volume of DMSO and added into water.

The influence of pH on the  $K_s$  value was studied in phosphate buffer (1 mM, water/DMSO, 98:2 v/v) at pH 7.34 and pH 5.5. Concentration of the porphyrins **2–4** was  $2.5 \times 10^{-6}$  mol/L, and concentration of the drugs varied from  $10^{-6}$  to  $10^{-4}$  mol/L. Hydrophobic drugs were dissolved in a small volume of DMSO and added into buffer.

**Preparation of the Complexes of the Porphyrins Carriers with the Drugs (Figure 1).** An amount of 11  $\mu$ L of a 28.6 mM DMSO solution of the respective drugs was added to 1 mL of 0.21 mM porphyrin (**1–4**) solution (water/DMSO, 98:2, v/v). The prepared solutions were vigorously stirred for 10 min, and then after 1 h of incubation at room temperature they were immediately used for subsequent experiments.

**Cell Cultures and in Vitro Experiments.** 4T1 (mouse mammary carcinoma) and K562 (human chronic myelogenous leukemia) cells were kept at exponential growth in RPMI 1640 medium with 10% fetal calf serum as described before.<sup>27</sup> For experiments  $(2-3) \times 10^5$  cells were seeded in 35 mm dishes and incubated overnight with the porphyrin-CD conjugates (**2–4**) (2.5–5  $\mu$ M), with particular cytostatics (0.5–10  $\mu$ M), or with their respective complexes. After incubation, cells were rinsed with PBS, supplied with fresh medium without phenol red for 1 h, and then illuminated with a 75 W halogen lamp with a band-pass filter (Andover, Salem, NH) with resulting wavelength 500–520 nm. The fluence rate at the level of the cell monolayer was 0.7 mW/cm<sup>2</sup>, and total light dose was 4 J/cm<sup>2</sup>. Following irradiation, the viability of post-PDT cultures was determined the next day by the Trypan blue exclusion method. Control “dark” experiments (without illumination) were performed in parallel.

**In Vivo Experiments.** BALB/c mice were subcutaneously transplanted with 4T1 mammary carcinoma cells as described previously.<sup>29</sup> When the tumor mass reached a volume of 200–300 mm<sup>3</sup> (about 7–10 days after transplantation), mice were injected with the porphyrin conjugates (**1–4**) (5 mg kg<sup>-1</sup>, iv) in a volume of 0.1 mL per 20 g mice, and 6 h later the tumor area (2 cm<sup>2</sup>) was irradiated with a 500–700 nm xenon lamp ONL 051 (maximum at 635 nm, Preciosa Crytur, Turnov, Czech Republic) with a total impact energy of 100 J cm<sup>-2</sup> and fluence rate of 200 mW cm<sup>-2</sup>. The control group represented mice exposed to the light without drug application. Each experimental group consisted of eight mice. All aspects of the animal experiment and husbandry were carried out in compliance with national and European regulations and were approved by the institutional committee.

**Acknowledgment.** This work was supported by grants from the Ministry of Education of the Czech Republic (Grants MSM 1M 6837805002, MSM6036137307,

MSM0021620857, AV0Z50520514; Projects LC 512, LC06077, and MSM6036137307) and by the Grant Agency of the Czech Republic (Grant 203/09/1311) and, in part, by Project AV0Z50520514 and Grant KAN200200651 awarded by the Grant Agency of the Academy of Sciences of the Czech Republic.

**Supporting Information Available:** Scheme of tested drugs, proposed model for pH dependent release, titration of **2–4** with cytostatic drugs, interaction of unconjugated porphyrin with  $\beta$ -cyclodextrin at various pH, interaction of **2** with  $\beta$ -cyclodextrin at various pH, absorption spectra of the porphyrin **2** in phosphate buffer, titration of **2** and **4** with HSA, ECD and fluorescence spectra of **2** in the presence of imatinib at various pH, titration of **2** with phenylalanine, absorption spectra of the **2**–paclitaxel complex in the presence of phenylalanine, stability of the complex **2**–paclitaxel at various pH, biolocalization of porphyrin–CD conjugates, influence of the one-shot porphyrin–CD–drug mediated therapy on C32 melanoma, log values of  $K_s$  for the porphyrin–CD complexes at various pH, NMR study of chemical shifts of doxorubicin in the presence of **3** and  $\gamma$ -CD, NMR spectra changes for imatinib with **2** and  $\beta$ -cyclodextrin, and obtained individual values for combined therapy used for statistical analysis. This material is available free of charge via Internet at <http://pubs.acs.org>.

## References

- (1) Kopecek, J.; Kopeckova, P.; Minko, T.; Lu, Z. R.; Peterson, C. M. Water soluble polymers in tumor targeted delivery. *J. Controlled Release* **2001**, *74*, 147–158.
- (2) Ladewig, M. S.; Karl, S. E.; Hamelmann, V.; Helb, H. M.; Scholl, H. P. N.; Holz, F. G.; Eter, N. Combined intravitreal bevacizumab and photodynamic therapy for neovascular age-related macular degeneration. *Graefes Arch. Clin. Exp. Ophthalmol.* **2008**, *246*, 17–25.
- (3) Lunardi, C. N.; Tedesco, A. C. Synergic photosensitizers: a new trend in photodynamic therapy. *Curr. Org. Chem.* **2005**, *9*, 813–821.
- (4) He, H.; Zhou, Y.; Liang, F.; Li, D.; Wu, J.; Yang, L.; Zhou, X.; Zhang, X.; Cao, X. Combination of porphyrins and DNA-alkylation agents: synthesis and tumor cell apoptosis induction. *Bioorg. Med. Chem.* **2006**, *14*, 1068–1077.
- (5) Uekama, K.; Hirayama, F.; Arima, H. Recent aspect of cyclodextrin-based drug delivery system. *J. Inclusion Phenom. Macrocyclic Chem.* **2006**, *56*, 3–8.
- (6) Rihova, B.; Strohalm, J.; Prausova, J.; Kubackova, K.; Jelinkova, M.; Rozprimova, L.; Sirova, M.; Plocova, D.; Etrych, T.; Subr, V.; Mrkvan, T.; Kovar, M.; Ulbrich, K. Cytostatic and immunomobilizing activities of polymer-bound drugs: experimental and first clinical data. *J. Controlled Release* **2003**, *91*, 1–16.
- (7) Vicent, M. J.; Greco, F.; Nicholson, R. I.; Paul, A.; Griffiths, P. C.; Duncan, R. Polymer therapeutics designed for a combination therapy of hormone-dependent cancer. *Angew. Chem., Int.* **2005**, *44*, 4061–4066.
- (8) Loftsson, T.; Masson, M. Cyclodextrins in topical drug formulations: theory and practice. *Int. J. Pharm.* **2001**, *225*, 15–30.
- (9) Hipler, U. C.; Schoenfelder, U.; Hipler, C.; Elsner, P. Influence of cyclodextrins on the proliferation of HaCaT keratinocytes in vitro. *J. Biomed. Mater. Res., Part A* **2007**, *83*, 70–79.
- (10) Uekama, K. Design and evaluation of cyclodextrin-based drug formulation. *Chem. Pharm. Bull.* **2004**, *52*, 900–915.
- (11) Cserhati, T.; Hollo, J. Interaction of taxol and other anticancer drugs with hydroxypropyl-beta-cyclodextrin. *Int. J. Pharm.* **1994**, *108*, 69–75.
- (12) Ceschel, G. C.; Mora, P. C.; Borgia, S. L.; Maffei, P.; Ronchi, C. Skin permeation study of dehydroepiandrosterone (DHEA) compared with its alpha-cyclodextrin complex form. *J. Pharm. Sci.* **2002**, *91*, 2399–2407.
- (13) Alcaro, S.; Ventura, C. A.; Paolino, D.; Battaglia, D.; Ortuso, F.; Cattel, L.; Puglisi, G.; Fresta, M. Preparation, characterization, molecular modeling and in vitro activity of paclitaxel–cyclodextrin complexes. *Bioorg. Med. Chem. Lett.* **2002**, *12*, 1637–1641.
- (14) Hagiwara, Y.; Arima, H.; Hirayama, F.; Uekama, K. Prolonged retention of doxorubicin in tumor cells by encapsulation of gamma-cyclodextrin complex in pegylated liposomes. *J. Inclusion Phenom. Macrocyclic Chem.* **2006**, *56*, 65–68.
- (15) Liu, Y.; Chen, Y. Cooperative binding and multiple recognition by bridged bis(beta-cyclodextrin)s with functional linkers. *Acc. Chem. Res.* **2006**, *39*, 681–691.
- (16) Liu, Y.; Chen, G. S.; Li, L.; Zhang, H. Y.; Cao, D. X.; Yuan, Y. J. Inclusion complexation and solubilization of paclitaxel by bridged bis(beta-cyclodextrin)s containing a tetraethylenepentaamino spacer. *J. Med. Chem.* **2003**, *46*, 4634–4637.
- (17) Liu, Y.; Yang, Y. W.; Yang, E. C.; Guan, X. D. Molecular recognition thermodynamics and structural elucidation of interactions between steroids and bridged bis(beta-cyclodextrin)s. *J. Org. Chem.* **2004**, *69*, 6590–6602.
- (18) Liu, Y.; Li, L.; Chen, Y.; Yu, L.; Fan, Z.; Ding, F. Molecular recognition thermodynamics of bile salts by beta-cyclodextrin dimers: factors governing the cooperative binding of cyclodextrin dimers. *J. Phys. Chem. B* **2005**, *109*, 4129–4134.
- (19) Allison, R. R.; Bagnato, V. S.; Cuenca, R.; Downie, G. H.; Sibata, C. H. The future of photodynamic therapy in oncology. *Future Oncol.* **2006**, *2*, 53–71.
- (20) Castano, A. P.; Mroz, P.; Hamblin, M. R. Photodynamic therapy and anti-tumour immunity. *Nat. Rev. Cancer* **2006**, *6*, 535–545.
- (21) Kral, V.; Kralova, J.; Kaplanek, R.; Briza, T.; Martasek, P. Quo vadis porphyrin chemistry? *Physiol. Res.* **2006**, *55*, S3–S26.
- (22) Kralova, J.; Koivukorpi, J.; Kejik, Z.; Pouckova, P.; Sievaenen, E.; Kolehmainen, E.; Kral, V. Porphyrin–bile acid conjugates: from saccharide recognition in the solution to the selective cancer cell fluorescence detection. *Org. Biomol. Chem.* **2008**, *6*, 1548–1552.
- (23) Wu, J. J.; Ma, H. L.; Mao, H. S.; Wang, Y.; Jin, W. J. Investigation on disassociation of porphyrin J-aggregates induced by  $\beta$ -cyclodextrins using absorption and fluorescence spectroscopy. *J. Photochem. Photobiol., A* **2005**, *173*, 296–300.
- (24) Luca, G.; Romeo, A.; Scolaro, L. M. Aggregation properties of hyperporphyrins with hydroxyphenyl substituents. *J. Phys. Chem. B* **2006**, *110*, 14135–14141.
- (25) Banfi, S.; Caruso, E.; Caprioli, S.; Mazzagatti, L.; Canti, G.; Ravizza, R.; Gariboldi, M.; Monti, E. Photodynamic effects of porphyrin and chlorin photosensitizers in human colon adenocarcinoma cells. *Bioorg. Med. Chem.* **2004**, *12*, 4853–4860.
- (26) Samaroo, D.; Vinodu, M.; Chen, X.; Drain, C. M. meso-Tetra(pentafluorophenyl)porphyrin as an efficient platform for combinatorial synthesis and the selection of new photodynamic therapeutics using a cancer cell line. *J. Comb. Chem.* **2007**, *9*, 998–1011.
- (27) Synytsya, A.; Kral, V.; Synytsya, A.; Volka, K.; Sessler, J. L. In vitro interaction of macrocyclic photosensitizers with intact mitochondria: a spectroscopic study. *Biochim. Biophys. Acta, Gen. Subj.* **2003**, *1620*, 85–96.
- (28) Kral, V.; Rusin, O.; Charvatova, J.; Anzenbacher, P.; Fogl, J. Porphyrin phosphonates: novel anionic receptors for saccharide recognition. *Tetrahedron Lett.* **2000**, *41*, 10147–10151.
- (29) Kralova, J.; Synytsya, A.; Pouckova, P.; Koc, M.; Dvorak, M.; Kral, V. Novel porphyrin conjugates with a potent photodynamic antitumor effect: differential efficacy of mono- and bis-beta-cyclodextrin derivatives in vitro and in vivo. *Photochem. Photobiol.* **2006**, *82*, 432–438.
- (30) Zaruba, K.; Vasek, P.; Kral, V. Study of molecular recognition of 5,10,15,20-tetrakis-(pentafluorophenyl)porphyrin- $\beta$ -cyclodextrin conjugate covalently immobilized on a silica surface. *Supramol. Chem.* **2004**, *16*, 529–536.
- (31) Rusin, O.; Hub, M.; Kral, V. Novel water-soluble porphyrin-based receptors for saccharide recognition. *Mater. Sci. Eng.* **2001**, *C18*, 135–140.
- (32) Kralova, J.; Briza, T.; Moserova, I.; Dolensky, B.; Vasek, P.; Pouckova, P.; Kejik, Z.; Kaplanek, R.; Martasek, P.; Dvorak, M.; Kral, V. Glycol porphyrin derivatives as potent photodynamic inducers of apoptosis in tumor cells. *J. Med. Chem.* **2008**, *51*, 5964–5973.
- (33) Hosseini, A.; Hodgson, M. C.; Tham, F. S.; Reed, C. A.; Boyd, P. D. V. Tapes, sheets, and prisms. Identification of the weak C–F interactions that steer fullerene–porphyrin cocrystallization. *Cryst. Growth Des.* **2006**, *6*, 397–403.
- (34) Toth, G.; Bowers, S. G.; Truong, A. P.; Probst, G. The role and significance of unconventional hydrogen bonds in small molecule recognition by biological receptors of pharmaceutical relevance. *Curr. Pharm. Des.* **2007**, *13*, 3476–3493.
- (35) Puglisi, A.; Purrello, R.; Rizzarelli, E.; Sortino, S.; Vecchio, G. Spectroscopic and self-association behavior of a porphyrin- $\beta$ -cyclodextrin conjugate. *New J. Chem.* **2007**, *31*, 1499–1506.
- (36) Leng, X.; Choi, Ch.-F.; Lo, P.-Ch.; Dennis, K. P. Assembling a mixed phthalocyanine–porphyrin array in aqueous media through host–guest interactions. *Org. Lett.* **2007**, *9*, 231–234.



- (37) Lang, K.; Kral, V.; Kapusta, P.; Kubat, P.; Vasek, P. Photoinduced electron transfer within porphyrin–cyclodextrin conjugates. *Tetrahedron Lett.* **2002**, *43*, 4919–4922.
- (38) Vinodu, M.; Goldberg, I. Synthesis and versatile supra-molecular self-assembly of the 5,15-bis(4-hydroxyphenyl)-10,20-bis(4-carboxyphenyl)porphyrin scaffold. *CrystEngComm* **2004**, *6*, 215–220.
- (39) Lazzeri, D.; Durantini, E. N. Synthesis of *meso*-substituted cationic porphyrins as potential photodynamic agents. *ARKIVOC* **2003**, *10*, 227–239.
- (40) Lang, L.; Kral, V.; Kapusta, P.; Kubat, P.; Vasek, P. Photoinduced electron transfer within porphyrin–cyclodextrin conjugates. *Tetrahedron Lett.* **2002**, *43*, 4919–4922.
- (41) Kralova, J.; Dvorak, M.; Koc, M.; Kral, V. p38 MAPK plays an essential role in apoptosis induced by photoactivation of a novel ethylene glycol porphyrin derivative. *Oncogene* **2008**, *27*, 3010–3020.
- (42) Zimmermann, A.; Walt, H.; Haller, U.; Baas, P.; Klein, S. D. Effects of chlorin-mediated photodynamic therapy combined with fluoropyrimidines in vitro and in a patient. *Cancer Chemother. Pharmacol.* **2003**, *51*, 147–154.